International Journal of Adhesion & Adhesives 67 (2016) 86–93

Contents lists available at ScienceDirect

International Journal of Adhesion & Adhesives

journal homepage: www.elsevier.com/locate/ijadhadh

Strength of cylindrical butt joints bonded with epoxy adhesives under combined static or high-rate loading

S. Murakami [a], Y. Sekiguchi [b], C. Sato [b,*], E. Yokoi [c], T. Furusawa [c]

[a] Graduate School, Tokyo Institute of Technology, 4259 Nagatsuta, Midori-ku, Yokohama 226-8503, Japan
[b] Precision and Intelligence Laboratory, Tokyo Institute of Technology, 4259 Nagatsuta, Midori-ku, Yokohama 226-8503, Japan
[c] Automobile R&D Center, Honda R&D Co., Ltd., 4630 Shimotakanezawa, Haga-machi, Haga-gun, Tochigi 321-3393, Japan

ARTICLE INFO

Available online 30 December 2015

Keywords:
(A) Toughened adhesive
(B) Steels
(C) Joint design
(C) Stress analysis

ABSTRACT

The influence of loading rates and the combined stress states of tension and shearing on the strength, strain, and absorbed energy of an adhesively bonded joint was experimentally investigated. Cylindrical butt joint specimens were prepared and strength tests were performed on the specimens with a servo-controlled hydraulic testing machine that combined tension and torsion loading. Two types of epoxy adhesives, ductile and brittle, were applied to the specimens. The tests were performed under a quasi-static condition of 6.67×10^{-2} MPa/s and a high-rate loading condition of 1.00×10^{3} MPa/s. The results of the combined loading tests showed that the states of the fractured surfaces were not affected by the loading rates. As for the ratio of tensile and shear loading, adhesive failure tended to partially occur when the ratio of shear loading was very high. The strength points for the specimens bonded with each adhesive were distributed in a stress plane of tension and shearing and could be fitted with a curve that was described by an equation with exponential parameters that were not influenced by the strain rate; however, other parameters that described the intercepts were influenced. The failure strains and absorbed energies for the brittle adhesive were slightly dependent on the strain rate, but this dependency was unclear for the ductile adhesive.

1. Introduction

The reduction of CO_2 emissions is an important environmental protection issue, and reducing the weight of vehicles is an effective and versatile method for resolving this problem. Automobile and aircraft components are consequently being constructed of lighter and higher-strength materials such as high-strength steel, aluminum alloys and carbon fiber reinforced plastics [1–3]. In addition, it has been predicted that the use of different materials within a structure, i.e., multi-materials, will increase in the future. Adhesive bonding is a suitable method for attaching joints in a multi-material structure. Compared with mechanically fastened or welded joints, adhesively bonded joints can reduce the product weight and increase productivity in terms of costs and production time. The adhesives used for bonding structural members are typically called structural adhesives. Richard reported on the properties and usage of structural adhesives [4].

Adhesively bonded joints in a structure may be subjected to a combination of tensile and shear loads. It is thus important to investigate the effects of combined loading states on the strength of these joints. It is possible to apply combined loading to a specimen through various test methods. For instance, combined loading tests were performed with an Arcan apparatus [5–7] on cylindrical butt-joint specimens [8–10]. Although an Arcan apparatus is convenient to use with a universal testing machine, it possesses an inherent problem of stress concentration. The use of cylindrical butt-joint specimens can precisely measure the strength of a joint under combined loading conditions.

The strength of an adhesively bonded joint at a high strain rate is crucial to automotive applications because car structures are subjected to impact loadings in crash scenarios. There has been significant research conducted on adhesive properties in high-rate loading using various methods [11–19]. The most popular method to measure the impact strength of a material is the Split Hopkinson Bar Test [20–22]. This method, however, does not easily measure the strength of an adhesively bonded joint under combined loading conditions, as few studies have been conducted for these loading conditions [23].

The energy absorbed by an adhesively bonded joint is important because it is closely related to the ductility of the joint. Adams et al. investigated the strengths of block impact specimens and measured their energy absorption [24]. In terms of joint fracture, a

* Corresponding author. Tel./fax: +81 45 924 5062.
E-mail address: csato@pi.titech.ac.jp (C. Sato).

http://dx.doi.org/10.1016/j.ijadhadh.2015.12.030
0143-7496/

critical energy release rate is another important value because it also characterizes the ductility of a joint, i.e., the absorbed energy per adhesion area. Adhesive layers are often represented by a cohesive zone model (CZM) to simulate crack propagation [25,26]. In these cases, the critical energy release rate of a joint is an essential parameter for the simulation. Various methods have been proposed to determine the critical energy release rate of an adhesively bonded joint [27–32], but these methods still have difficulties with complicated situations such as high-rate loadings in either mode II or a combined mode.

This paper presents a novel experimental method for measuring the strength of an adhesively bonded joint subjected to high-rate combined loading of tension and sharing using a servo-controlled hydraulic testing machine and a cylindrical butt-joint specimen bonded with adhesive. Through this method, uniformly-distributed tensile and shear stresses can be simultaneously applied to the joint in the specimen. The loading rate can be specified from a quasi-static to high-rate state because the hydraulic testing machine is specifically designed to work appropriately at a high speed. The deformation of the adhesive layer in the specimen was measured with an extensometer and the energy absorbed in the layer was calculated from the experimentally obtained load–displacement curve.

2. Experiment

2.1. Materials

The adherends in the joint specimen are made of S45C carbon steel. Two types of adhesive—one-component ductile epoxy adhesive (XA7416, 3 M Japan Ltd., Tokyo, Japan) and a two-component brittle epoxy adhesive (DENATITE2204, Nagase ChemteX Co., Ltd., Osaka, Japan)—were selected for use in this study.

2.2. Specimen preparation

2.2.1. Bulk adhesive specimens

The mechanical properties of the adhesives were experimentally investigated through tensile tests of the bulk specimens. The geometry of the bulk specimens comprising the adhesives is shown in Fig. 1. The tensile tests were conducted with a mechanical testing machine (Autograph AGS-500A, Shimadzu Co., Ltd., Kyoto, Japan) at a crosshead speed of 0.5 mm/min.

2.2.2. Cylindrical butt-joint specimens

The geometry of a cylindrical butt-joint specimen is shown in Fig. 2. The adhesion surface for the adherend was treated with #600 sandpaper and degreased with acetone. An adhesive was applied to the adherends and they were bonded with the specially made jig shown in Fig. 3. A micrometer was installed at the upper part of the jig that was temporally fixed to the upper adherend with adhesive tape. The spindle of the micrometer met the lower part of the jig so that a proper thickness of the gap between the adherends could be obtained. The mechanism enabled us to control the thickness of the adhesive layer at an objective value of 0.3 mm. After bonding, XA7416 was cured at 140 °C for 20 min. and DENATITE2204 was cured 100 °C for 30 min. while being supported by the jig in a temperature chamber. The adherends and the thickness control jig were made from the same material—S45C. For this reason, any differences of bonding space between the adherends during heat curing would be minimal. Spew fillets around the joints were removed with an ultrasonic knife to control the stress concentration [33].

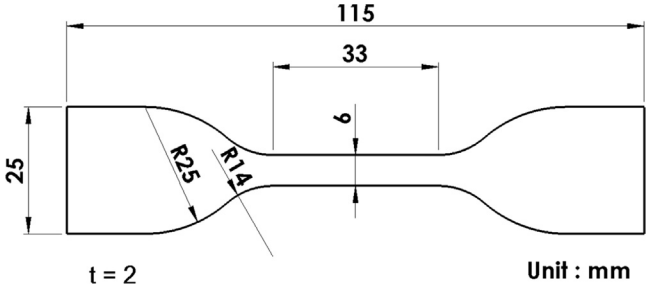

Fig. 1. Configuration and dimensions of bulk specimen made of adhesive.

2.3. Testing

Schematic illustrations of the hydraulic testing machine used for the study are shown in Figs. 4 and 5. The testing machine was originally developed by Shindo et al. [34] and based on a machine invented by Lindholm [35] that was modified by the authors. The machine has a hydraulic actuator with two oil chambers—one for tensile loading and the other for shear loading. The actuator is controlled with a pair of closed-loop feedback systems comprising a load cell, strain amplifiers, displacement sensors, electric circuits, and servo valves. The feedback control systems were only used for quasi-static tests because displacement control was possible when considering the response time. Because the control systems were not able to be utilized because of the slow response during high-rate loading, an open-loop control was employed. The increments of the actuator displacement rate were determined by preliminary tests aimed at objectively identifying the stress increment rate. The advantage of this testing machine is that both oil chambers in the actuator begin simultaneous loading when one of the loads exceeds the static friction; as a result, the synchronization of the tensile and torsional loading can be established, even for high-rate loading.

The loads applied to a specimen were measured with a specially made load cell from which tensile and torsional loads could be simultaneously measured. The deformation of the adhesive layer in a specimen was measured with the biaxial extensometer shown in Fig. 6, which utilized a pair of eddy current gap sensors placed in the axial and circumferential directions.

The specimens were tested under combined loading conditions in which two stress rates were selected: 6.67×10^{-2} MPa/s for the quasi-static condition and 1.00×10^{3} MPa/s for the high-rate condition. The tensile stress σ and shear stress τ in the adhesive layer were calculated by

$$\sigma = \frac{F}{\frac{\pi}{4}\left(d_o^2 - d_i^2\right)}, \quad \tau = \frac{T}{\frac{\pi}{16}\frac{d_o^4 - d_i^4}{d_o}}, \tag{1}$$

where F is the tensile load, T is the torque, d_o is the outer diameter ($=$ 26 mm) and d_i is the inner diameter ($=$20 mm) of the specimen. The tensile strain ε and shear strain γ were calculated from measured displacements with the biaxial extensometer by

$$\varepsilon = \frac{l_1}{t}, \quad \gamma = \frac{l_2}{t}, \tag{2}$$

where l_1 is the axial displacement, l_2 is the circumferential displacement at the outer diameter of the adherents, and t is the thickness of the adhesive layer. Absorbed energies, W_1 for tension and W_2 for shearing, were calculated by integrating each stress–displacement curve to the maximum displacements l_{1f} and l_{2f} with the following equations:

$$W_1 = \int_0^{l_{1f}} \sigma(x)dx, \quad W_2 = \int_0^{l_{2f}} \tau(x)dx. \tag{3}$$

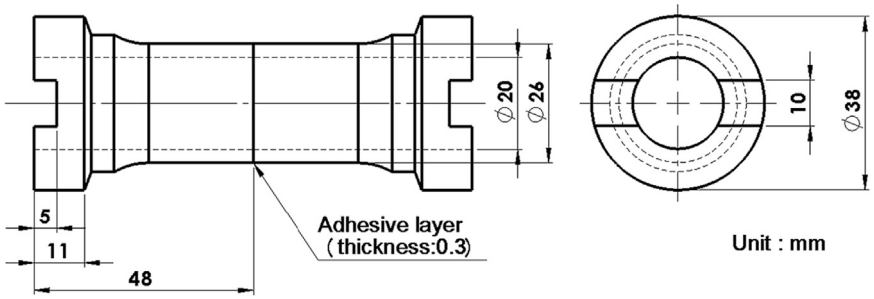

Fig. 2. Configuration and dimensions of cylindrical butt-joint specimen.

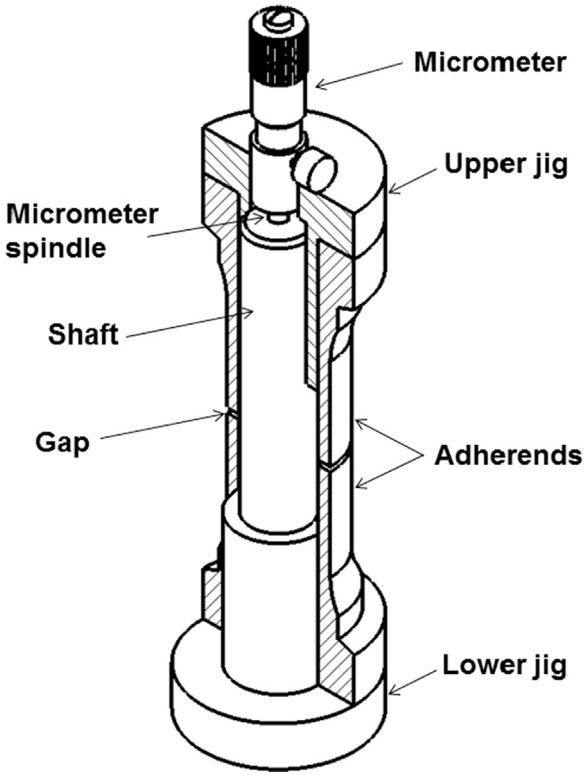

Fig. 3. Schematic illustration of jig for thickness control (cut model).

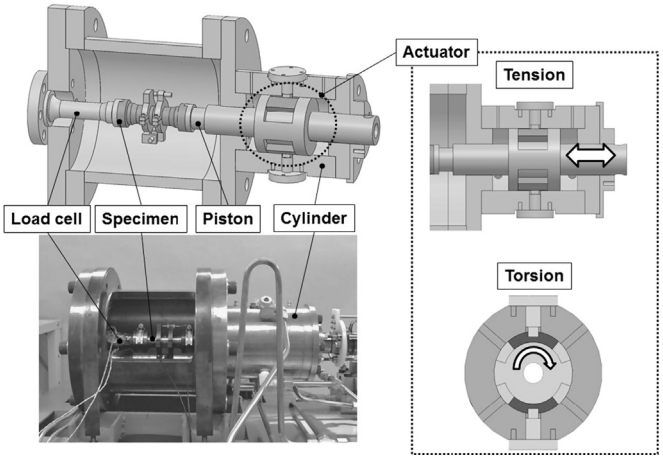

Fig. 4. Working principle of hydraulic testing machine for combined loading of tension and torsion.

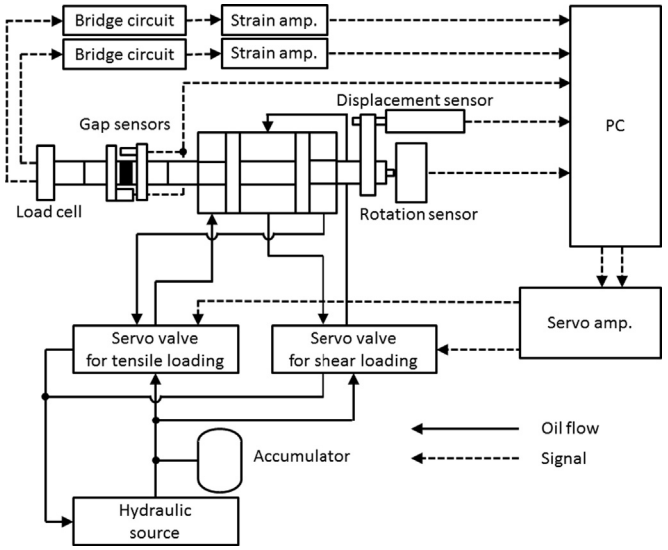

Fig. 5. Control system diagram of hydraulic testing machine.

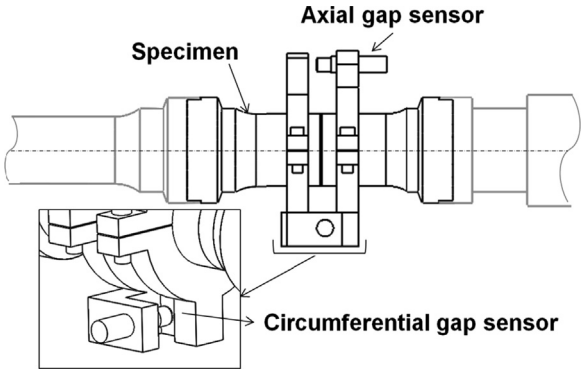

Fig. 6. Schematic illustration of biaxial extensometer.

The specimens were tested under combined loading conditions in which two stress increment rates were selected: 6.67×10^{-2} MPa/s for the quasi-static condition and 1.00×10^{3} MPa/s for the high-rate condition. In this study, a loading angle θ was used for the loading condition index. This leads to a ratio of tensile and shear stress calculated by the following equation:

$$\theta = \arctan\left(\frac{\tau}{\sigma}\right). \tag{4}$$

3. Results and discussion

3.1. Mechanical properties of adhesive bulk under quasi-static loading

The stress–strain diagrams of the bulk specimens made of the adhesives under quasi-static loading are shown in Fig. 7 and the mechanical properties obtained from the diagrams are summarized in Table 1. The tensile testing was conducted three times for each adhesive. The ductile adhesive XA7416 exhibited greater elongation and strength than the brittle adhesive DENATITE2204. In contrast, Young's modulus of DENATITE2204 was higher than that of XA7416.

3.2. Results of combined loading tests

Tables 2 and 3 show the results of the combined loading tests. The tensile and shear strengths were determined from the maximum tensile or shear stress point. If the times that indicated maximum tensile and shear stress occurred in different timing, then the time when the sums of the squares of tensile and shear stress was greatest was deemed the strength point. Cohesive failure occurred in the adhesive layers under most conditions of the combined loading tests. However, the failure locus moved toward an interface between the adhesive layer and the adherend with the increasing shear loading ratio. When the ratio of shear loading was high, adhesive failure predominantly occurred in the specimens bonded with XA7416, as shown in Fig. 8. Two types of failures can be observed in Fig. 8: a dominant adhesive failure on the interfaces and a partial cohesive failure connecting the interfaces across the adhesive layer. The latter may be due to initial cracks in the adhesive layer generated by a shearing load that propagated at an angle of 45 degrees from the interfaces. It was found that these fractured surfaces were affected not by the loading rate but rather by the ratio of tensile and shear loading for both the ductile and brittle adhesives.

The tensile stress–strain diagrams of adhesive layers in cylindrical butt-joint specimens are shown in Fig. 9. Each curve was plotted with the experimental data of the applied load to a specimen and displacement between the adherents of the specimen measured with the biaxial extensometer. These curves were smoothed by low-pass filtering to reduce noise in loads and displacements. The high-rate strength was 1.52 times greater than the quasi-static state for XA7416 and 1.40 times greater for DENATITE2204. The ductile adhesive XA7416 exhibited strain-rate dependency as the tensile strength and failure strain increased. In contrast, the failure strain did not increase for the brittle adhesive

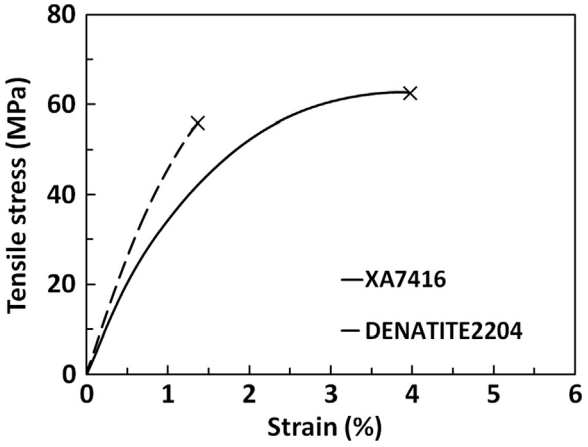

Fig. 7. Stress–strain curves of bulk specimens made of two types of adhesive.

Table 1
Mechanical properties of epoxy adhesives: XA7416 and DENATITE2204

Adhesive	Young's modulus [GPa]	Maximum stress [MPa]	Failure strain [%]
XA7416	4.53	62.0	4.10
DENATITE2204	5.34	47.7	1.15

DENATITE2204 but the tensile strength increased. The shear stress–strain diagrams of the cylindrical butt-joint specimens are shown in Fig. 10. The ductile adhesive XA7416 exhibited plastic deformation under both quasi-static and high-rate conditions, whereas the brittle adhesive DENATITE2204 behaved elastically in every loading case. The fracture point in time of a specimen bonded with XA7416 in high-rate loading was unclear because the load remained high and did not become zero after the fracture; this was due to friction between the fractured surfaces of the specimen. In this case, the fracture point of the specimen was determined from the time when the tensile displacement began to increase. Similar to the tensile tests, the shear strengths under high-rate loading were approximately 34% higher than those in the quasi-static tests for both XA7416 and DENATITE2204.

The tensile and shear strengths of the cylindrical butt-joint specimens are shown in Fig. 11 (a) and (b), in which a point indicates the strength of a specimen in a space of tensile and shear stresses. These strengths increased with rising loading rates for both adhesives. In this study, tensile stress was calculated from Eq. (1), which means that stresses in the adhesive layer were uniformly distributed. In fact, stress concentration occurred near the interface of the adherend and adhesive during tensile loading. Spaggiari and Dragoni et al. proposed geometry that reduced stress concentration and reported that tensile strength increased due to a relief groove [36–38]. This is likely to underestimate tensile strength; however, the relationship between stress concentration at the interface and fracture morphology, especially in the case of cohesive failure, would change case by case, and plastic deformation should exist near the edge of adhesive layer, which can reduce stress concentration, and the place where the initial crack was generated could not be determined from the fracture surface. Therefore, stress distribution was assumed to be uniform and the effect of stress concentration on tensile strength is not discussed in this paper. The strength points of an adhesive can be fitted by a curve plotted by using the following empirical equation for both quasi-static and high-rate loading cases:

$$\left(\frac{x}{a}\right)^m + \left(\frac{y}{b}\right)^m = 1, \tag{5}$$

where strength parameters a and b are determined from the tensile and shear strengths of each adhesive and the exponential parameter m is determined by the least square method applied to the experimental data. The values of the parameters, which are shown in Table 4, indicate that a and b are significantly affected by strain rate and m is quite insensitive. These results suggest that the exponent parameter m, which is influential in the shape of strength distribution in a tensile-shear plane, was primarily determined by adhesive properties.

The failure strains of the cylindrical butt-joint specimens are shown in Fig. 12 (a) and (b). The failure strains of XA7416 showed significant scatter due to the difficulty in determining the fracture as previously mentioned, although they appear to depend on loading rates. In contrast, DENATITE2204 exhibited little strain-rate dependency and the points in failure strain aligned linearly. In this study, the precise tendency of failure strain could not be determined, particularly for XA7416. Although May et al. studied the properties of a crash-optimized epoxy adhesive using tube specimens and found that failure strain decreased with rising

Table 2
Results of combined loading tests bonded with XA7416.

Loading rate	Loading angle [deg.]	Tensile strength [MPa]	Shear strength [MPa]	Failure strain in tension [%]	Failure strain in shear [%]	Absorbed energy in tension [kJ/m^2]	Absorbed energy in shear [kJ/m^2]
Quasi-static	0.28	61.8	0.31	2.68	−0.30	0.20	0.00
Quasi-static	2.53	65.5	2.89	3.83	0.33	0.37	0.00
Quasi-static	1.09	67.5	0.55	4.06	0.06	0.36	0.00
Quasi-static	18.0	61.0	19.9	2.15	2.85	0.16	0.11
Quasi-static	36.4	53.0	39.0	5.27	19.6	0.52	1.97
Quasi-static	35.1	55.4	38.9	8.38	10.4	1.00	0.89
Quasi-static	41.0	46.1	40.0	1.94	12.5	0.16	1.19
Quasi-static	45.0	41.7	41.8	8.71	21.1	0.85	2.29
Quasi-static	60.8	25.5	45.6	0.94	21.1	0.05	2.54
Quasi-static	64.2	22.9	47.4	3.06	26.1	0.17	3.25
Quasi-static	77.8	10.9	50.7	2.33	32.1	0.06	4.14
Quasi-static	89.1	0.8	52.6	0.77	49.5	0.01	6.98
Quasi-static	−80.9	−8.6	53.6	-2.15	34.8	0.04	5.94
High-rate	0.09	90.0	0.14	3.62	0.09	0.39	0.00
High-rate	0.27	109	0.52	6.26	0.51	1.04	0.00
High-rate	15.5	92.1	25.5	3.55	3.69	0.40	0.18
High-rate	37.6	69.7	53.7	3.35	17.2	0.40	2.23
High-rate	37.2	72.1	54.8	1.41	19.2	0.12	2.25
High-rate	36.8	73.6	55.1	6.54	18.0	0.99	2.10
High-rate	57.9	38.1	60.9	2.01	26.6	0.12	4.31
High-rate	79.6	12.9	70.5	0.64	58.1	0.02	10.0
High-rate	65.6	30.2	66.7	4.61	50.7	0.34	7.94
High-rate	−83.6	−7.99	71.1	−1.41	32.2	0.02	5.75

Table 3
Results of combined loading tests bonded with DENATITE2204.

Loading rate	Loading angle [deg.]	Tensile strength [MPa]	Shear strength [MPa]	Failure strain in tension [%]	Failure strain in shear [%]	Absorbed energy in tension [kJ/m^2]	Absorbed energy in shear [kJ/m^2]
Quasi-static	4.24	47.6	3.53	1.82	0.30	0.10	0.00
Quasi-static	−0.11	43.8	−0.08	3.02	−0.09	0.20	0.00
Quasi-static	1.33	55.6	1.29	4.44	0.60	0.43	0.00
Quasi-static	48.5	37.7	24.8	2.61	3.42	0.16	0.15
Quasi-static	55.4	27.8	40.3	1.56	6.87	0.06	0.43
Quasi-static	65.9	21.0	47.1	1.38	8.86	0.04	0.71
Quasi-static	67.7	18.4	44.8	1.41	7.99	0.02	0.69
Quasi-static	78.6	10.4	51.5	2.07	9.97	0.04	0.87
Quasi-static	−82.3	−7.13	52.7	−1.47	11.3	0.03	1.15
High-rate	0.31	66.9	0.37	2.61	0.33	0.19	0.00
High-rate	−0.16	71.8	−0.08	4.24	−0.18	0.48	0.00
High-rate	0.73	67.4	0.86	3.69	0.27	0.39	0.00
High-rate	16.6	55.6	16.5	2.88	2.25	0.18	0.06
High-rate	25.4	50.9	24.0	2.53	3.33	0.22	0.12
High-rate	52.2	36.6	47.2	1.47	5.82	0.10	0.47
High-rate	62.8	23.1	55.1	0.67	7.65	0.03	0.72
High-rate	70.9	21.8	62.8	1.49	11.35	0.03	1.16
High-rate	−81.6	−10.4	70.9	−0.54	12.58	−0.03	1.63

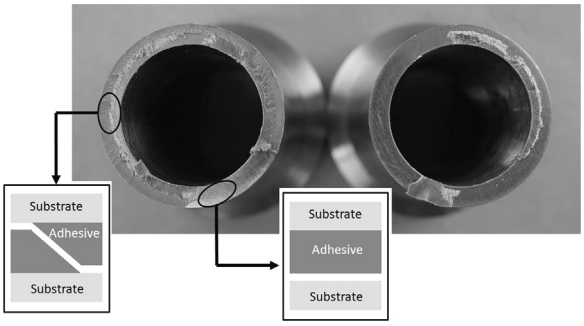

Fig. 8. Fractured surface (Adhesive: XA7416, condition: high-rate, shear loading).

strain rate [39], the increase of loading rate may have decreased failure strain in our experiments.

The energy absorbed by the joint in each cylindrical butt-joint specimen is plotted in Fig. 13 (a) and (b). The ductile adhesive

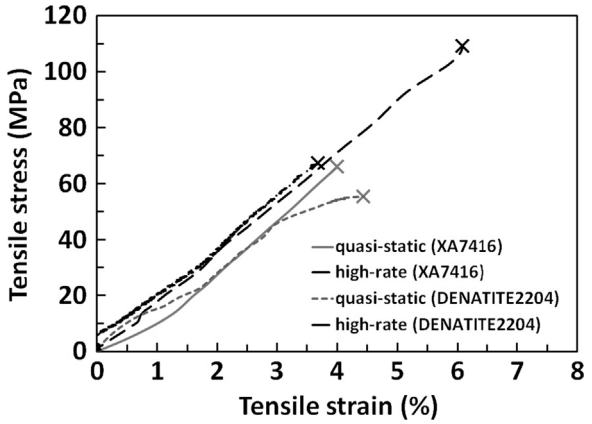

Fig. 9. Tensile stress–strain curves of adhesive layers in cylindrical butt-joint specimens.

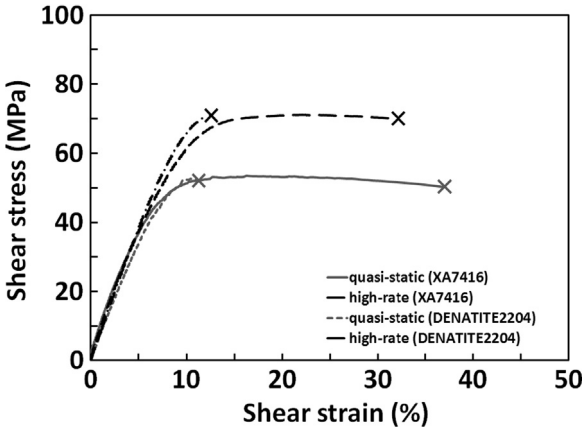

Fig. 10. Shear stress–strain curves of adhesive layers in cylindrical butt-joint specimens.

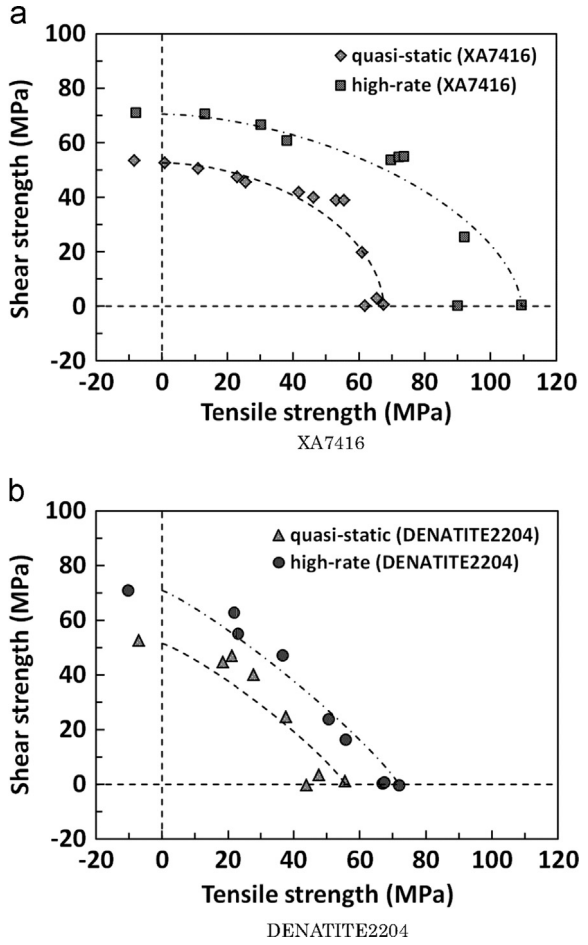

Fig. 11. Biaxial strengths of cylindrical butt joints bonded with adhesives XA7416 and DENATITE2204 under quasi-static and high-rate loading conditions.

Table 4
Parameters *a*, *b* and *m* for epoxy adhesives: XA7416 and DENATITE2204.

Adhesive	Loading rate	Tensile strength *a* [MPa]	Shear strength *b* [MPa]	Exponential parameter *m*
XA7416	Quasi-static	67.5	53.6	1.85
	High-rate	109	71.1	1.71
DENATITE2204	Quasi-static	55.6	52.7	1.17
	High-rate	71.8	70.9	1.14

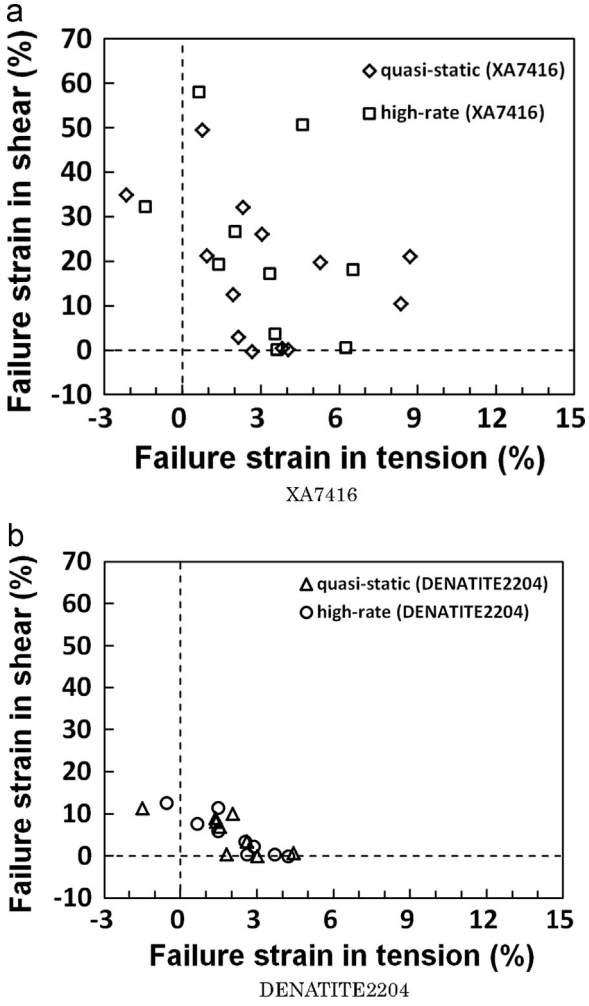

Fig. 12. Biaxial failure strains of cylindrical butt joints bonded with adhesives XA7416 and DENATITE2204 under quasi-static and high-rate loading conditions.

XA7416 absorbed more energy than the brittle adhesive DENATITE2204. The absorbed energies in shearing were greater than those in tension. However, the influence of loading rates on the absorbed energies is unclear, particularly for XA7416. For DENATITE2204, the failure strains did not vary even though the strength increased. Although the absorbed energy increased as a consequence, the resulting difference was slight.

4. Conclusions

In this study, the influence of loading rates and the combined stresses of tension and shearing on the strengths of adhesively bonded joints was experimentally investigated using cylindrical butt-joint specimens bonded with two types of epoxy adhesive—ductile and brittle. Quasi-static and high-rate loading was applied to the specimens using a hydraulic testing machine for combined testing. The failure strains and absorbed energies of the specimens were also measured. The obtained results in the research can be summarized as follows:

(1) Fractured surfaces were primarily influenced by a ratio of tensile and shear stresses. The influence of loading rates was trivial. Adhesive failure predominantly occurred in the ductile adhesive when the ratio of shear loading was high.
(2) The strength under high-rate loading of a cylindrical butt joint was greater than that under quasi-static loading for both the

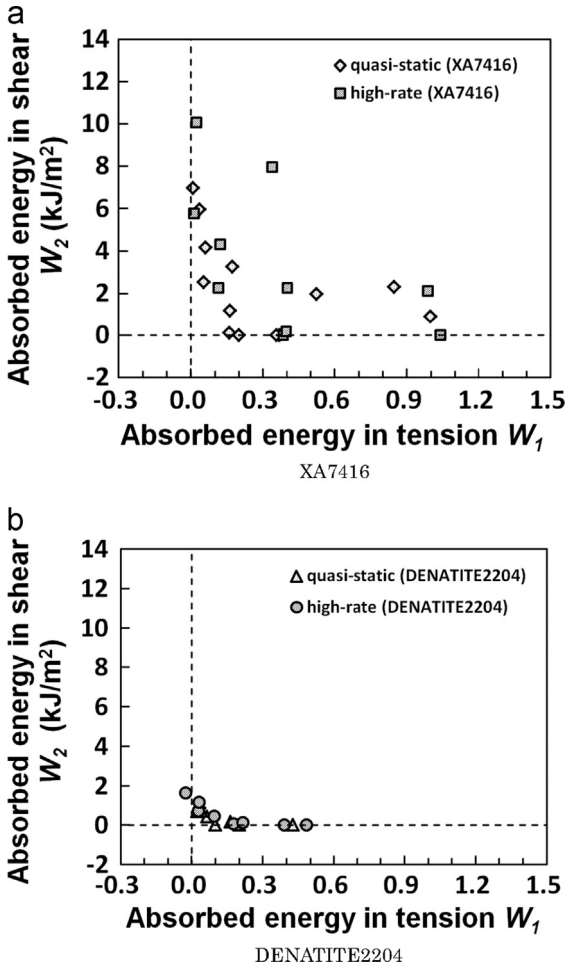

Fig. 13. Absorbed energies of cylindrical butt joints bonded with adhesives XA7416 and DENATITE2204 under quasi-static and high-rate loading conditions.

ductile and brittle adhesives. The strengths of the specimens, which were plotted in a tensile-shear space, were able to be fitted by a curve defined by an empirical equation whose exponential parameters were not influenced by strain rates, although the strength parameters depended on the rates.

(3) The failure strain and absorbed energy of the brittle adhesive exhibited little strain-rate dependency. However, the failure strain and absorbed energy of the ductile adhesive were not precisely determined because the fracture of the cylindrical butt-joint specimens bonded with the adhesive was difficult to detect.

References

[1] Loureiro AL, da Silva LFM, Sato C, Figueiredo MAV. Comparison of the mechanical behaviour between stiff and flexible adhesive joints for the automotive industry. J Adhes 2000;86:765–87. http://dx.doi.org/10.1080/00218464.2010.482440.

[2] Michalos G, Makris S, Papakostas N, Mourtzis D, Chryssolouris G. Automotive assembly technologies review: challenges and outlook for a flexible and adaptive approach. CIRP J Manuf Sci Technol 2010;2:81–91. http://dx.doi.org/10.1016/j.cirpj.2009.12.001.

[3] Goede M, Stehlin M, Rafflenbeul L, Kopp G, Beeh E. Super Light Car—lightweight construction thanks to a multi-material design and function integration. Eur Transp Res Rev 2009;1:5–10. http://dx.doi.org/10.1007/s12544-008-0001-2.

[4] Pethrick RA. Design and ageing of adhesives for structural adhesive bonding—a review. Proc Inst Mech Eng Part L 2015;5:349–79. http://dx.doi.org/10.1177/1464420714522981.

[5] Cognard JY, Créac'hcadec R, Sohier L, Davies P. Analysis of the nonlinear behavior of adhesives in bonded assemblies—comparison of TAST and Arcan tests. Int J Adhes Adhes 2008;28:393–404. http://dx.doi.org/10.1016/j.ijadhadh.2008.04.006.

[6] Cognard JY, Badulescu C, Maurice J, Créac'hcadec R, Carrére N, Vedrine P. On modelling the behavior of a ductile adhesive under low temperatures. Int J Adhes Adhes 2014;48:119–29. http://dx.doi.org/10.1016/j.ijadhadh.2013.09.014.

[7] Bresson G, Jumel J, Shanahan MER, Serin P. Strength of adhesively bonded joints under mixed axial and shear loading. Int J Adhes Adhes 2012;35:27–35. http://dx.doi.org/10.1016/j.ijadhadh.2011.12.006.

[8] Yoshida T, Takiguchi M, Yoshida F. Strength of highly ductile acrylic adhesive in butt-joint under combined tension and torsion. Key Eng Mater 2004;274-276:993–8. http://dx.doi.org/10.4028/www.scientific.net/KEM.274-276.993.

[9] Ikegami K, Kajiyama M, Kamiko S, Shiratori E. Experimental studies of the strength of an adeshive joint in a state of combined stress. J Adhes 1979;10:25–38. http://dx.doi.org/10.1080/00218467908544609.

[10] Castagnetti D, Spaggiari A, Dragoni E. Effect of bondline thickness on the static strength of structural adhesives under nearly-homogeneous shear stresses. J Adhes 2011;87:780–803. http://dx.doi.org/10.1080/00218464.2011.597309.

[11] Sato C, Ikegami K. Dynamic deformation of lap joints and scarf joints under impact loads. Int J Adhes Adhes 2000;20:17–25. http://dx.doi.org/10.1016/S0143-7496(99)00010-X.

[12] Maheri MR, Adams RD. Determination of dynamic shear modulus of structural adhesives in thick adherend shear test specimens. Int J Adhes Adhes 2002;22:119–27. http://dx.doi.org/10.1016/S0143-7496(01)00043-4.

[13] Kadioglu F, Adams RD. Flexible adhesive for automotive application under impact loading. Int J Adhes Adhes 2015;56:73–8. http://dx.doi.org/10.1016/j.ijadhadh.2014.08.001.

[14] Hayashida S, Sugaya T, Kuramoto S, Sato C, Mihara A, Onuma T. Impact strength of joints bonded with high-strength pressure-sensitive adhesive. Int J Adhes Adhes 2015;56:61–72. http://dx.doi.org/10.1016/j.ijadhadh.2014.09.005.

[15] Kihara K, Isono H, Yamabe H, Sugibayashi T. A study and evaluation of the shear strength of adhesive layers subjected to impact loads. Int J Adhes Adhes 2003;23:253–9. http://dx.doi.org/10.1016/S0143-7496(03)00004-6.

[16] Sankar HR, Adamvalli M, Kulkarni PP, Parameswaran V. Dynamic strength of single lap joints with similar and dissimilar adherends. Int J Adhes Adhes 2015;56:46–52. http://dx.doi.org/10.1016/j.ijadhadh.2014.07.014.

[17] Pohlit DJ, Dillard DA, Jacob GC, Starbuck JM. Evaluating the rate-dependent fracture toughness of an automotive adhesive. J Adhes 2008;84:143–63. http://dx.doi.org/10.1080/00218460801952825.

[18] Challita G, Othman R, Casari P, Khalil K. Experimental investigation of the shear dynamic behavior of double-lap adhesively bonded joints on a wide range of strain rates. Int J Adhes Adhes 2011;31:146–53. http://dx.doi.org/10.1016/j.ijadhadh.2010.11.014.

[19] Zhang F, Yang X, Xia Y, Zhou Q, Wang HP, Yu TX. Experimental study of strain rates effects on the strength of adhesively bonded joints after hygrothermal exposure. Int J Adhes Adhes 2015;56:3–12. http://dx.doi.org/10.1016/j.ijadhadh.2014.07.008.

[20] Goglio L, Peroni L, Peroni M, Rossetto M. High strain-rate compression and tension behaviour of an epoxy bi-component adhesive. Int J Adhes Adhes 2008;28:329–39. http://dx.doi.org/10.1016/j.ijadhadh.2007.08.004.

[21] Yokoyama T. Determination of impact shear strength of adhesive joints with the split hopkinson bar. Key Eng Mater 1998;145-9:317–22. http://dx.doi.org/10.4028/www.scientific.net/KEM.145-149.317.

[22] Yokoyama T, Nakai K. Determination of impact tensile properties of structural epoxy adhesive butt joints using a hat-shaped specimen. J Phys IV Fr 2006;134:789–95. http://dx.doi.org/10.1051/jp4:2006134122.

[23] Sato C, Ikegami K. Strength of adhesively-bonded butt joints of tubes subjected to combined high-rate loads. J Adhes 1999;70:57–73. http://dx.doi.org/10.1080/00218469908010487.

[24] Adams RD, Harris JA. A critical assessment of the block impact test for measuring the impact strength of adhesive bonds. Int J Adhes Adhes 1996;16:61–71. http://dx.doi.org/10.1016/0143-7496(95)00050-X.

[25] Marzi S, Hesebeck O, Brede M, Kleiner F. A rate-dependent cohesive zone model for adhesively bonded joints loaded in mode I. J Adhes Sci Technol 2009;23:881–98. http://dx.doi.org/10.1163/156856109X411238.

[26] Alfano M, Furgiuele F, Leonardi A, Maletta C, Paulino GH. Cohesive zone modeling of mode i fracture in adhesive bonded joints. Key Eng Mater 2007;348-9:13–6. http://dx.doi.org/10.4028/www.scientific.net/KEM.348-349.13.

[27] Blackman BRK, Kinloch AJ, Sanchez FSR, Teo WS, Williams JG. The fracture behaviour of structural adhesives under high rates of testing. Eng Fract Mech 2009;76:2868–89. http://dx.doi.org/10.1016/j.engfracmech.2009.07.013.

[28] Blackman BRK, Kinloch AJ, Taylor AC, Wang Y. The impact wedge-peel performance of structural adhesives. J Mater Sci 2000;35:1867–84. http://dx.doi.org/10.1023/A:1004793730352.

[29] Chen Z, Adams RD, da Silva LFM. Fracture toughness of bulk adhesives in mode I and III and curing effect. Int J Fract 2011;167:221–34. http://dx.doi.org/10.1007/s10704-010-9547-9.

[30] da Silva LFM, de Magalhães FACRG, Chaves FJP, de Moura MFSF. Mode II fracture toughness of a brittle and a ductile adhesive as a function of the adhesive thickness. J Adhes 2010;86:891–905. http://dx.doi.org/10.1080/00218464.2010.506155.

[31] Ikegami K, Fujii T, Kawagoe H, Kyogoku H, Motoie K, Nohno K, Sugibayashi T, Yoshida F. Benchmark tests on adhesive strengths in butt, single and double lap joints and double-cantilever beams. Int J Adhes Adhes 1996;16:219–26. http://dx.doi.org/10.1016/0143-7496(95)00051-8.

[32] Yang QD, Thouless MD, Ward SM. Elastic–plastic mode-II fracture of adhesive joints. Int J Solids Struct 2001;38:3251–62. http://dx.doi.org/10.1016/S0020-7683(00)00221-3.
[33] Adams RD, Coppendale J, Peppiatt NA. Stress analysis of axisymmetric butt joints loaded in torsion and tension. J Strain Anal Eng Des 1978;13:1–10. http://dx.doi.org/10.1243/03093247V131001.
[34] Shindo A, Sato M, Yamashita A, Hagiwara T. Trial manufacture of dynamic combined load testing machine and a few experiments on mild steel. Proc Jpn S Mech Eng Kansai Branch 234th Meet 1975;754-10:45–7.
[35] Lindholm US, Yeakley LM. A dynamic biaxial testing machine. Exp Mech 1967;7:1–7. http://dx.doi.org/10.1007/BF02326833.
[36] Castagnetti D, Spaggiari A, Dragoni E. Robust shape optimization of tubular butt joints for characterizing thin adhesive layers under uniform normal and shear stresses. J Adhes Sci Technol 2010;24:1959–76. http://dx.doi.org/10.1163/016942410X507687.
[37] Spaggiari A, Dragoni E. Experimental tests on tubular bonded butt specimens: effect of relief grooves on tensile strength of the adhesive. J Adhes 2012;88:499–512. http://dx.doi.org/10.1080/00218464.2012.660831.
[38] Spaggiari A, Castagnetti D, Dragoni E. Mixed-mode strength of thin adhesive flims: experimental characterization through a tubular specimen with reduced edge effect. J Adhes 2013;89:660–75. http://dx.doi.org/10.1080/00218464.2012.750243.
[39] May M, Hesebeck O, Marzi S, Böhme W, Lienhard J, Kilchert S, Brede M, Hiermaier S. Rate dependent behavior of crash-optimized adhesives—experimental characterization, model development and simulation. Eng Fract Mech 2015;133:112–37. http://dx.doi.org/10.1016/j.engfracmech.2014.11.006.